Synthetic Self-Assembled Materials in Biological Environments

Versluis, Frank; van Esch, Jan H.; Eelkema, Rienk

DOI
10.1002/adma.201505025

Publication date
2016

Document Version
Accepted author manuscript

Published in
Advanced Materials

Citation (APA)
Versluis, F., van Esch, J. H., & Eelkema, R. (2016). Synthetic Self-Assembled Materials in Biological Environments. *Advanced Materials*, *28*(23), 4576–4592. https://doi.org/10.1002/adma.201505025

DOI: 10.1002/adma. 201505025

Synthetic Self-Assembled Materials in Biological Environments

By *Frank Versluis,* Jan H. van Esch* and *Rienk Eelkema**

Dr. F. Versluis, Prof. J. H. van Esch and Dr. R. Eelkema
Advanced Soft Matter Group, Department of Chemical Engineering,
Delft University of Technology, 2628BL, Delft, The Netherlands
E-mail:f.versluis@tudelft.nl, r.eelkema@tudelft.nl

Abstract

Synthetic self-assembly has long been recognized as an excellent approach for the formation of ordered structures on the nanoscale. Although the development of synthetic self-assembling materials has often been inspired by principles observed in nature (e.g. the assembly of lipids, DNA, proteins), until recently the self-assembly of synthetic molecules has mainly been investigated ex vivo. The past few years however, have witnessed the emergence of a research field in which synthetic, self-assembling systems are used that are capable of operating as bioactive materials in biological environments. This progress report is devoted to this up-and-coming field which has the potential of becoming a key area in chemical biology and medicine. We identify and discuss two main categories of applications of self-assembly in biological environments, namely as therapeutic and imaging agents. Within these categories we will discuss key concepts such as triggers and molecular constraints for in vitro/in vivo self-assembly and the mode of interaction between the assemblies and the biological materials.

1. Introduction

This progress report deals with the self-assembly of synthetic molecules in biological environments, which find application as imaging and therapeutic agents. Self-assembly is defined as the spontaneous organization of molecular components into ordered architectures,

and has proven in recent years to be a highly successful approach towards the development of bioactive materials. The main reason for this is that self-assembly is the most feasible method for the fabrication of ordered molecular structures on the nanoscale.[1] As these structures are held together by non-covalent interactions, careful balancing of the intra- and intermolecular interactions within the assemblies can lead to the formation of materials that are relatively robust while retaining the ability to respond appropriately to external stimuli.[2] Moreover, self-assembly is highly flexible, enabling control over the formed structures by the mixing of various similar self-assembling building blocks.[3] Historically, self-assembly processes in nature (e.g. lipid membranes, actin filaments) have inspired scientists to design synthetic self-assembly systems in an attempt to both understand natural systems and develop novel materials with properties that were otherwise unattainable. Taking all these factors into account, self-assembly as a methodology promises myriads of applications in biology and medicine, including drug delivery systems, radically different ways to influence cellular processes and molecular imaging in living subjects. However, most reported work is performed ex vivo and only recently have the first examples of synthetic self-assembling systems in living environments started to appear. The main reason for this is that translating the self-assembly of molecular components from the controlled and diluted conditions in a test tube to the highly complex and dynamic environment of living systems is a non-trivial matter.

Using synthetic self-assembly in living systems poses several challenges and restricts the range of building blocks that can be used. First, self-assembly needs to take place in a bioorthogonal and biocompatible way, selectively providing the desired interaction of the synthetic with the biological material without disturbing either the self-assembly process or biological functions. Second, the self-assembling molecules and aggregated structures should not be susceptible to rapid degradation, although self-assembly itself typically enhances the chemical stability of the molecular components against proteolytic degradation. Third,

accurate spatial control over the self-assembly process is often required. Consequently, this poses the challenge of inducing assembly at the area of interest. Various strategies have been developed to turn inactive species into self-assembling molecules including concentration, pH,[4] light,[5] incorporation of cleavable self-assembly blocking group[6] or chemical reactions.[7] If in situ self-assembly methods are employed, the biodistribution, uptake, circulation and toxicity of the building blocks themselves become highly important. Importantly, the first in vivo/in vitro self-assembly efforts have emerged in recent years, enabling spatial control over synthetic self-assembly in living environments. Moreover, the development of reactions that can take place under physiological conditions and do not unselectively react with common biomolecules,[8] thereby triggering self-assembly, has been crucial.

We have identified two main fields within which self-assembly in biological environments finds application, namely as imaging agents and as therapeutic agents, and this progress report is organized accordingly. In the imaging section, self-assembly based approaches for obtaining high contrast of fluorescence intensity in cellular systems are discussed. We will first describe examples where enzymes remove protecting groups from precursors, yielding self-assembling molecules that form ordered structures. Subsequently, systems are discussed that effectively operate as on/off fluorescent probes. Interestingly, whereas one type becomes fluorescent upon self-assembly, the other type is turned on via disassembly of 'silent' aggregates. In the therapeutic agents section, we first devote a segment to the creation of a synthetic extracellular matrix around specific cell types. Next, we discuss systems based on self-assembling drug conjugates as efficient, high loading, drug delivery vehicles. The final segment concerns the use of peptide amphiphile based fibers that act as therapeutic agents. In introducing the different segments, we will put emphasis on a number of features displayed by the self-assembling systems, including: 1) what induces self-assembly, 2) what are the constraints on the molecular design due to biological influences, 3) what type of structures are

typically formed (e.g. micelles, fibers etc.) and how does that morphology aid their functioning.

In this progress report we will focus on recent and exciting examples of self-assembly based approaches towards the formation of materials that can be used as imaging tools or therapeutics. Other areas of research which fall within the bounds of 'synthetic self-assembly in biological environments,' including tissue engineering[9] and supramolecular systems that can bind to cells through multivalent interactions[10] will not be discussed here, as recent reviews are available. After reading this progress report, we hope to have elucidated why the use of self-assembly in chemical biology and medicine deserves attention, what the current state of the art is with respect to methodology and applications and finally what progress can be expected in the coming years.

2. Imaging agents

Fluorescence imaging is of enormous importance in elucidating biological structure, function and mechanisms.[11] To acquire high resolution images of living biological systems, obtaining a high ratio of contrast between the region of interest and its surroundings is pivotal. This requires a high local concentration of fluorescent groups at the biological target, whereas the surroundings remain silent. In the following paragraphs, two self-assembly based methods to perform this intricate task are described. In the first approach, fluorescent precursors are used that self-assemble after enzymatic cleavage of a protecting group, limiting self-assembly to the vicinity of the enzyme. In the second approach, amphiphiles containing protein ligands aggregate in aqueous media to give non-fluorescent aggregates due to self-quenching. Upon the binding of the ligand to the protein, the aggregates break up, self-quenching is relieved and the target proteins are illuminated.

2.1 Enzyme triggered self-assembly

A highly potent strategy to develop imaging tools is the use of precursor molecules which undergo self-assembly upon the cleavage of a protecting group by an enzyme. Upon

dispersion of the non-self-assembling precursor in aqueous media, a weak and homogeneously fluorescent solution is obtained. Enzymatic cleavage of the protecting group leads to self-assembly of the fluorescent molecule, for example into fibers. Now, fluorescence is stringently restricted to the aggregates, yielding high contrast between the formed self-assembled materials and their surroundings **(Fig. 1)**.

A difficult but crucial objective is to have self-assembly take place specifically at the region of interest. As the protecting group is enzymatically cleaved, self-assembly will take place in the vicinity of the enzyme, enabling accurate spatial control over self-assembly. Interestingly, by tuning this protecting group, various enzymes can be targeted selectively, allowing for the imaging of subcellular structures and cellular processes. An important prerequisite for this imaging technique is that the precursor molecules do not self-assemble, whereas enzymatic cleavage of the protecting group leads to rapid self-assembly (at the enzyme location) into highly fluorescent aggregates. This effect is often achieved using a highly hydrophilic protecting group, which upon removal leads to a large reduction in hydrophilicity of the remaining molecule. The upcoming examples will show that cellular substructures and cellular processes can be visualized using this methodology.

Highly interesting examples of enzyme triggered self-assembly in living cells were reported by the group of Rao. In their first contribution in 2010, a chemical reaction between 2-cyanobenzothiazole (CBT) and D-cysteine was used to trigger self-assembly **(Fig. 2)**, which proceeds under physiological conditions.[12] Both thiol and amino groups of the cysteine were protected, via a disulfide bond and by the peptide sequence RVRR, respectively. Finally, the linker R^3 could be used to install biotin, allowing for high resolution TEM imaging through the addition of streptavidin-coated gold particles, or a fluorescent reporter group. Through test tube reactions, the authors showed that the addition of Furin or tris(2-carboxyethyl)phosphine (TCEP) to either amino or thiol protected **1** yielded oligomeric products, which subsequently self-assembled into a variety of morphologies such as fibers and snowflakes.

Next, enzyme triggered self-assembly of derivatives of **1** in living cells was attempted. For visualization purposes, the lysine linker (R^3) was functionalized with fluorescein isothiocyanate (FITC). This monomer was added to cultured MDA-MB-468 cells and after 2 h of incubation, fluorescence images were recorded **(Fig.2C)**. Importantly, it was found that the condensation reaction occurred near the Golgi bodies (stained separately with a Golgi marker), which is known to be the predominant location of Furin.[13] A control experiment in which the protecting peptide sequence was scrambled, making it unsusceptible to cleavage by Furin, revealed very weak and homogeneous fluorescence throughout the cell. These findings indicate that enzyme triggered self-assembly can be used to target self-assembly with subcellular precision, revealing the location of the enzymes.

In a following contribution by the Rao group,[14] a derivative of **1** was labelled with a gadolinium (Gd) complex and the authors protected the thiol group using a disulfide bond. The diffusion of this compound into MDA-MB-468 cells led to the reduction of the disulfide bond by GSH and subsequent self-assembly yielded nanoparticles, rich in Gd. These nanoparticles could subsequently be imaged using MRI (magnetic resonance imaging), as they displayed enhanced T_1 relaxivity compared to the molecularly dispersed components. One drawback of using derivatives of **1** was that the CBT group can also react with endogenous cysteine. In a subsequent contribution of the Rao group, this was improved upon by using 2-cyano-6-hydroxyquinoline (CHQ) instead of CBT, showing a 480-fold decrease in the second order rate constant with respect to free cysteine.[15] Furthermore, glycine linkers were introduced, to promote intramolecular cyclization, upon which the condensation products self-assembled into fibrous structures. Similarly to their previous work, the authors protected the thiol and amino groups and added the resulting compound to living cells. Cleavage of the blocking groups by Furin and GSH sparked intramolecular condensation, leading to self-assembly close to the Golgi body. Next, this macrocyclization strategy was used to assemble Gd rich particles in reducing (e.g. cellular) environments.[16] Overall, these

works nicely demonstrate that self-assembly in living cells can be controlled by using protecting groups that can be cleaved by endogenous enzymes. As a result of self-assembly, high local concentrations of probes are obtained, yielding excellent contrast in biological samples.

The examples discussed in this section show that enzyme triggered self-assembly can be used for the formation of aggregates which are restricted to specific subcellular structures, based on the notion that specific enzymes reside predominantly in certain organelles. As these aggregates contain high concentrations of fluorescent groups, they are excellent imaging tools. In the next section, this approach is taken one step further, allowing for the visualization of a specific cellular process.

The group of Rao further developed their enzyme triggered self-assembly method to visualize cellular processes in vivo, in real-time.[17] The cellular process that was targeted was apoptosis (cell death), which is highly relevant as it enables the detailed investigation of the efficacy of anti-cancer drugs. The general approach is shown in **Fig. 3**. In a molecule denoted C-SNAF, cleavage of the peptide segment DEVD by caspases and reduction of the disulfide bond, resulted in cyclization between the C-SNAF cyanobenzothiazole (CBT) and cysteine groups.[17] After cyclization, the compound self-assembles into highly fluorescent nanospheres with an approximate diameter of 175 nm. Importantly, caspases are activated upon apoptosis and therefore the combination of these two triggers for cyclization and self-assembly ensure that self-assembly of C-SNAF can only occur inside apoptotic cells. Upon self-assembly, the local concentration of the fluorescent probe Cy5.5 is markedly increased, supplying contrast between the apoptotic cells and the extracellular space. Interestingly, the aggregates are contained in the cells for extended periods of time, whereas the monomeric species quickly diffuse in and out of cells that do not express caspases. Therefore, precursors that enter apoptotic cells are trapped in aggregates as additional precursors enter the apoptotic

cells. This mechanism yields a high concentration of fluorescent aggregates in the target cells, whereas healthy cells contain very few fluorescent precursors.

To check if C-SNAF could specifically label apoptotic cancer cells, apoptosis was induced in HeLa cells through the addition of staurosporine (STS). Subsequently, C-SNAF was added and visualized by flow-cytometry and fluorescence microscopy, revealing that self-assembly occurred specifically in apoptotic HeLa cells. Viable HeLa cells could not be visualized by C-SNAF and a range of control compounds (inhibiting peptide cleavage or by methylating the thiol) confirmed that the proposed mechanism of 1) peptide cleavage, 2) disulfide cleavage, 3) cyclization and 4) self-assembly did indeed take place. In a next step, tumor bearing mice were treated with the anti-cancer drug DOX and C-SNAF was administered intravenously. Non-invasive longitudinal fluorescence imaging was used to determine the location and aggregation state of C-SNAF. The authors observed that the fluorescence intensity was mainly concentrated in the tumor tissue of the DOX treated mice, whereas this effect was not observed in tumor bearing mice that did not receive DOX. Overall, this study convincingly shows that C-SNAF undergoes enzyme mediated self-assembly in apoptotic cells, enabling the non-invasive visualization of dying cells in vivo, in real-time. In a follow-up paper, the Rao group showed that this principal can be extended to Gd based MRI probes.[18] Here, caspases trigger the self-assembly of the MRI probe. Upon intracellular self-assembly the authors observe enhanced r_1 relaxivity and an enhancement of the magnetic resonance signal, showing that the MRI sensitive material is capable of visualizing cellular processes in vivo. Using a similar strategy, the Rao group synthesized a ^{18}F labelled molecule that can undergo enzyme catalyzed self-assembly in living cells.[19] Using tumor bearing mice, it was shown that this compound can be used as an activatable positron emission tomography (PET) tracer, capable of visualizing apoptotic cells in DOX treated mice. In conclusion, enzyme triggered self-assembly has been shown to be capable of tracking the cellular apoptosis process in vivo. By carefully selecting protecting groups on precursors for self-assembly, it was possible to

localize self-assembly to apoptotic cells, based on activation of certain enzymes in dying cells. Self-assembly efficiently traps monomers inside aggregates in the desired cells, enabling the selective targeting of the imaging material. Furthermore, the basic molecular design can be modified to target various proteins, by changing the protecting groups. Through this strategy, other proteins and cellular proteins can be accessed.

2.2 Enzyme triggered self-assembly based on/off probes

In the preceding section, the self-assembly of fluorescent molecules generated highly fluorescent aggregates. For certain probes however, it has been observed that high concentrations lead to self-quenching.[20] To prevent this, specific fluorescent probes have been developed that are silent when they are molecularly dispersed, only to light up upon aggregation. These probes have been denoted aggregation induced emission (AIE) probes and can give excellent contrast due to the fact that it is only fluorescent in the aggregated state.[21] This phenomenon is observed when tetraphenylethylene derivatives are used and is thought to be based on a restriction of intramolecular rotations of this construct in the aggregated state. This effect prohibits energy dissipation through mechanisms other than radiation, leading to high quantum yields in aggregated states. To turn fluorescence on in a controlled and targeted fashion, a basic requirement therefore is that molecular construct is highly water soluble, to prevent aggregation and concomitant fluorescence prior to target recognition. Turning aggregation and fluorescence of the AIE probe on can be performed via enzymatic cleavage of a hydrophilic protecting group as described earlier.

In a joint effort, the groups of Tang and Liu aimed to visualize apoptosis,[22] using an AIE fluorescent probe and similar overall strategy as described earlier by the Rao group. The AIE moiety tetraphenylethene (TPE) was covalently conjugated to the DEVDK peptide segment which can be cleaved by caspases. Caspases cleave the peptide bond between asparagine and lysine, triggering the self-assembly of the remaining K-TPE, which was expected to yield

highly fluorescent aggregates. Apoptotic MCF-7 cells were highly fluorescent after the incubation with the peptide-TPE conjugate. To show that the mechanistic underpinnings are based on cleavage of the peptide by caspases, both healthy cells and cells that had been treated with a caspase inhibitor showed little fluorescence intensity. Importantly, no washing steps were required in the procedure, due to the silent nature of the peptide-TPE in the unaggregated state. These results show that this compound can be used to screen possible inducers for apoptosis in vitro. Subsequently, the in vivo efficacy of this approach was investigated.[23] In the molecular design, the lysine residue was removed and the PTE probe was replaced by tetraphenylethene pyridinium (PyTPE). Whereas TPE has an excitation wavelength of 312 nm, PyTPE excites at 405 nm, enabling in vivo imaging as light of this wavelength is much less harmful to living subjects. Tumour bearing mice were injected with the DEVD-PyrTPE conjugate and the apoptosis inducer staurosporine (STS) was also added. It was observed that fluorescence levels were low in normal tissues, whereas the tumor region was clearly marked by fluorescence. Omitting the addition of STS resulted in similar fluorescence levels for the tumour and normal tissues. These findings show that the probe can enter cells of living mice, after which peptide cleavage takes place specifically in tumor cells that are undergoing apoptosis. This is followed by self-assembly of the Pyr-TPE segments, yielding highly fluorescent aggregates. It follows that these probes can be effectively used to visualize apoptotic cells.

In another example of this principle, Liu, Yang and Ding showed that AIE probes can be used to visualize bacterial proteins.[24] Here, a far-red/near-infrared (FR/NIR) probe was coupled to two peptide segments, capable of binding two proteins (TIP-1 and ULD-TIP-1). Whereas the probe by itself is virtually silent, binding to the protein induces a dramatic increase in fluorescence. The compound was added to E.coli bacteria that expressed either TIP-1 or ULD-TIP-1 and significant fluorescence was observed, only in the bacteria. Interestingly, TIP-1 contains one binding site for the probe and the complex self-assembled into spherical

aggregates, whereas ULD-TIP-1 contains four binding sites and upon addition of the probe, fiber networks were observed, with the probe acting as a crosslinker between the protein units.

2.3 Turning a fluorescent probe on through protein mediated disassembly

As noted, specially designed AIE probes become fluorescent upon aggregation. More commonly, self-assembly of fluorescent amphiphiles leads to a certain degree of self-quenching of fluorescence, due to the high local concentration of probe molecules. Although aggregation induced quenching (AIQ) is typically regarded as a nuisance, the Hamachi group cleverly used this effect to their advantage. Efficient self-quenching yields aggregates which are silent, however, upon the disassembly of the aggregates, self-quenching is cancelled and fluorescent monomers are acquired. To trigger disassembly, protein ligands were incorporated in the design, yielding a fluorescent probe that is turned on upon protein binding. Typically, the aggregates that these type of materials form have to be of the micellar kind, as larger aggregates (e.g. vesicles) do not disassemble very easily. Micelles are much more dynamic, therefore enabling rapid breakup of the assemblies and efficient targeting of proteins. To facilitate both assembly and disassembly, the overall hydrophobicity of the probe is crucial. The molecule needs to be quite hydrophobic to ensure tight aggregation and efficient self-quenching, yet still be able to disassemble upon reaching the target protein.

In a first contribution of the Hamachi group, their main aim was to visualize membrane bound folate receptors.[25] Using a molecular construct that contained a ligand that has affinity for folate receptors (methotrexate, MTX) and the hydrophobic fluorescent probe BODIPY, it was observed that upon dispersion in aqueous solution, BODIPY fluorescence was effectively quenched due to aggregation. Upon the addition of folate receptors, aggregate break-up resulted in a 23-fold fluorescence increase. However, upon addition to cells, the BODIPY-MTX conjugates were able to penetrate the cell membrane and unspecific binding to the cell membrane was observed through folate independent fluorescence increase. These results indicate that the overall construct is too hydrophobic to specifically detect receptors present in

cell membranes. However, switching to the hydrophilic fluorescein probe resulted in a conjugate that did not display efficient quenching of fluorescence as aggregation was diminished. Installing an additional hydrophobic dipeptide (di-(4-trifluoromethyl-phenylalanine) in the linker region was sufficient to effectively quench fluorescence, because of enhanced aggregation. Importantly, upon the addition of folate receptors, MTX binding to the receptor ensued, leading to the disassembly of the aggregates and an 8-fold increase in fluorescence. Upon the addition of BODIPY-dipeptide-MTX to live KB cells (a subline of HeLa cells), strongly fluorescent membranes were observed **(Fig. 4)**. To show that this result was not due to unspecific binding, competing folate receptors were added, decreasing the fluorescence intensity of the cellular membranes dramatically. This example highlights a crucial characteristic of self-assembly, the ability of controlling the physical properties of self-assembled materials based on the design of the molecular components. Carbonic anhydrase, another membrane protein that is overexpressed in tumors, was targeted using a similar molecular construct. The authors show that these proteins can also be visualized, exploiting a benzenesulfonamide ligand.[25]

In a subsequent contribution, the Hamachi group attempted to visualize several *intra*cellular proteins using the approach described above. In principal, the molecular design allows for the incorporation of a wide range of protein ligands and therefore, the presence or absence of proteins can be investigated, based on the fluorescence output. Moreover, once binding of the fluorescent probes to the enzymes has been observed through fluorescence increase, this approach can be used to screen various substances for their interactions with intracellular proteins, as strong binding of these substances will lead to a significant reduction in fluorescence intensity. In this contribution, a molecule was synthesized composed of an MTX ligand, and a tetramethylrhodamine (TMR) fluorophore, connected by a hydrophobic spacer.[26] The ligand binds to the cytosolic enzyme dihydrofolate reductase (eDHFR) and using a HeLa cell line that overexpresses GFP-fused eDHFR (HeLa-DG), addition of the

probe molecule yielded strong TMR fluorescence throughout the cell. In a control experiment in which normal HeLa cells were used that did not overexpress GFP-eDHFR, very weak fluorescence was observed. Remarkably, upon the addition of trimethoprim, which binds strongly to eDHFR, the fluorescence of the probe molecule was largely removed. This finding indicates that the probe molecules are not only removed from the binding site of eDHFR, but are also capable of reassembling within the living cell. Next, the endogenous cytosolic protein hCAII was targeted. MTX was replaced by a benzenesulfonamide ligand, which binds specifically to hCAII. The self-assembly and concomitant fluorescence quenching of this new compound was confirmed and the self-assembled material was added to MCF-7 cells which naturally expresses hCAII. After 4h incubation, the cells lit up brightly, indicating cellular uptake of the molecular probe and disassembly of the aggregates. To confirm that the increase of fluorescence was due to specific binding of the probe ligand with hCAII, a strong inhibitor for this protein was added, resulting in near complete removal of fluorescence. The apparent intracellular reassembly of this material shows that the disassembly was triggered by specific interactions between the ligand and the enzyme. Finally, this process was repeated, enabling the targeting of the tumor related HSP90 protein.

In a highly interesting account, the Yang group combined the quenching effects of Förster Resonance Energy Transfer (FRET) and aggregation.[27] The fluorophore FITC was conjugated to dabcyl, which quenches its fluorescence. As a linker between this FRET pair the peptide sequence that is recognized and cleaved by caspases (produced by apoptotic cells) was included, making the fluorescence of these compounds responsive to caspase enzymatic action. To initiate and control the extent of aggregation, varying numbers of phenyl alanine residues were added to the spacer sequence. The authors observed that the fluorescence of strongly aggregating compounds was more effectively quenched than of non-aggregating compounds, demonstrating the AIQ effect. As anticipated, the dabcyl group efficiently quenched fluorescence and it was observed that the combined FRET and aggregation effects

on fluorescence quenching were stronger than the individual effects. Upon the addition of these compounds to apoptotic cells, the cells lit up brightly due to the cleavage of the dabcyl group and phenyl alanines from the fluorescent group, eliminating both quenching effects.

Overall, self-assembly based strategies are highly promising for the development of imaging tools. Most importantly, employing aggregation induced emission and aggregation induced quenching, fluorescent probes have been created that can be efficiently turned on and off. More traditional fluorescent probes that rely only on for example protein recognition give relatively high background fluorescence due to unbound probes. When using hydrophilic probes that target membrane proteins for example, this can be remedied by using washing steps, but with hydrophobic probes for intracellular or in vivo use however, this solution is not feasible. These problems are overcome using self-assembly based turn on/off probes. Moreover, several enzymes have been identified which are capable of turning fluorescence on through cleavage of a self-assembly blocking group. This approach enables the in vivo visualization of proteins, which can reveal the location of certain proteins or, alternatively, cellular processes such as apoptosis.

3. Therapeutic agents

Using self-assembly based methods, therapeutic effects can be obtained via three radically different mechanisms, along which lines the categories in the following segment are defined . In the first part, systems are described that are capable of forming intracellular or extracellular fibrous networks. The fibers are formed in situ, upon the enzymatic cleavage of a hydrophilic protecting group from a soluble precursor. Self-assembly of dense networks in/around cells is thought to inhibit diffusion of biomolecules through the cell. As communication between cells and organelles is vital for cellular survival, the reduced metabolic activity could potentially lead to cell death. The second therapeutic mechanism is based on interactions between ex vivo formed peptide amphiphile fibers with cellular membranes. As peptides can be easily synthesized[28] and their interactions are fairly well understood,[29] this allows for the

systematic investigation of the effect of peptide amphiphile assemblies on the viability, differentiation and growth of cells. The final mechanism combines the more traditional use of small organic drug molecules to target for example proteins, carbohydrates or DNA, with advantageous characteristics of self-assembly. As drug molecules are typically hydrophobic, covalent conjugation of a hydrophilic moiety (e.g. a peptide) leads to the formation of an amphiphile that can undergo self-assembly. By using a labile linker, drug delivery systems can be developed with high drug loading and efficient delivery into cells.

3.1 Using fiber networks to selectively kill malignant cells

One of the most fascinating self-assembly based methods to construct therapeutic materials is the in situ formation of fiber networks in or around cells.[30] Typically, the molecules that have been used to achieve this are peptide-based hydrogelators. Upon dispersion in aqueous solvent, these compounds self-assemble into long fibers that eventually form a network, able to retain solvent. In principle, control over the location of formation of the gel network can be achieved using a protecting group which prevents gelation. Upon cleavage of the self-assembly blocking group, the gelator is formed and self-assembly ensues. The precursor molecules do not contain a direct targeting agent and will therefore diffuse into all cells. However, the blocking group can be chosen such that it is cleaved by enzymes that are only present in malignant cells (e.g. cancer or bacteria). Only upon entry into the targeted cell, the precursors are stripped of their blocking groups and fibers will be formed which are incapable of diffusing out of the cells. Therefore this approach enables the build-up of fibers inside the targeted cells. Moreover, by targeting enzymes that are present in the cell membrane, fiber networks around cells can be created and as this is thought to hinder the diffusion of molecules in or out of cells and communication with other cells, it is also expected to lead to cell death.

Typically, phosphate groups have been used as blocking groups,[30a] as they 1) bear a negative charge which dramatically increases the hydrophilicity of the molecule, thereby preventing self-assembly and 2) can be cleaved by cells that express increased levels of phosphatases. Exploring the self-assembly of synthetic nanostructures inside living cells is highly interesting as it might provide an attractive strategy to develop anti-cancer therapeutics and antibiotics.

3.2 In situ hydrogelation to kill cells

In 2007, the Xu group pioneered enzyme triggered self-assembly of fiber networks in a biological environment. In their first contribution, they aimed to form hydrogels inside living bacteria, using a phosphate protected naphthalene-Phe-Phe-Tyr hydrogelator **(Fig. 5)**.[31]

The authors first showed ex vivo that alkaline phosphatases are capable of cleaving the phosphate group from precursor **2**, yielding hydrogels based on **3**. Next, the precursor was added to E. coli bacteria that were genetically modified to overexpress phosphatases, and was incubated for 24h. The cells were subsequently lysed, revealing the presence of **3** in concentrations above the minimum gelation concentration. Next, the cells were suspended via sonication and the suspension readily formed a hydrogel. TEM analysis of this sample revealed the existence of fibers with similar dimensions as observed ex vivo. Moreover, only bacteria that were incubated with **2** could be stained with congo red, a dye which is known to stain fibrous materials. As a concequence of hydrogelation precursor **2** was shown to be highly toxic for E. coli bacteria that overexpress phosphatases, with IC_{50} values of 20 μg/mL.

In a similar study of the Xu group, HeLa cells were targeted for hydrogelation. Here, a negatively charged succinic acid protecting/solubilizing group was used, coupled on one side to the hydroxy-derived naphthalene-Phe-Phe hydrogelator via an ester moiety. As HeLa cells produce high levels of esterases, this design allows for the formation of the fiber networks specifically at HeLa cells. Again, hydrogelation was observed in the presence of the cells,

which also turned out to be detrimental to cell viability. Conversely, healthy mammalian cells (NIH3T3) were not affected, due to lower levels of cytosolic esterases.[32]

These two examples nicely show that through the choice of the self-assembly blocking group, cell specific nanostructures can be formed. However, the mechanism of cellular entry of the precursor, the location of self-assembly (at the membrane or intracellularly), as well as the mechanism through which these fiber networks induce apoptosis were not addressed. This was improved upon in a next contribution of the Xu group, where fiber formation was visualized.[33] Towards this aim, the authors synthesized a fluorescently labelled precursor for hydrogelation **(Fig. 6)**. The addition of the hydrogelator precursor at a concentration of 500 μM to cultured HeLa cells showed the formation of highly dense fiber networks inside the cells after only 5 minutes. This remarkable result shows that the anionic species bypasses endocytosis and is lipophilic enough to simply diffuse over the cellular membrane. Interestingly, the spatial profile of the self-assembled structures are consistent throughout different cells, with the nanofibers being present in the vicinity of the nucleus and in the region of the endoplasmic reticulum (ER).[34] To confirm that self-assembly originates at the ER, the phosphatase PTP1B that is known to reside in the ER was inhibited. After 1 hour of co-incubation of the inhibitor and precursor, the inhibition of PTP1B resulted in significantly lower NBD fluorescence. This is a clear indication of decreased fiber formation, as NBD fluorescence is increased within the hydrophobic fibers. Overall, these results shows that the phosphatase PTP1B plays an important role in the dephosphorylation and subsequent self-assembly into nano-fibers.

In a following paper, the Xu group reported the formation of pericellular fiber networks around HeLa cells.[35] Here, a small D-peptide derivative (naphthalene-Phe-Phe-Tyr) was used and modified with a negatively charged phosphate group **(Fig. 7)**. Rather remarkably, it was observed earlier that the addition of nap-Phe-Phe-Lys(NBD)-Tyr (all L-amino acids) to

HeLa cells gave dense fiber networks inside cells within 5 minutes,[33] whereas here, the structurally similar D-peptide yields pericellular fiber networks around HeLa cells. The difference might be caused by the NBD functionalized lysine residue, or the different stereochemistry. In a typical experiment, compound **D-1** was added to HeLa cells, which are known to overexpress surface and secretory phosphatases. These enzymes are capable of recognizing and subsequently cleaving phosphate groups and therefore, the addition of **D-1** to cancer cells leads to the formation of hydrogelator **D-2** close to the membrane of the cells, yielding synthetic fibers around the cells. Whereas gel formation around HeLa cells could be observed with the naked eye, addition of **D-2** at similar concentrations to HeLa cells did not lead to gel formation. This result strongly indicates that **D-1** is converted to **D-2** mainly at the cell surface, leading to locally increased concentrations of the hydrogelator, enabling self-assembly of this compound into fibers. Through the use of cryo-SEM and TEM, the fibrous structures around the HeLa cells were visualized, highlighting the difference between typical HeLa cells which display a smooth surface, and cells incubated with **D-1**, which revealed the presence of porous structures at the cell surface. Importantly, non-cancer cells (i.e. Ect1/E6E7) did not catalyze fiber formation around the cellular membranes, as confirmed by confocal microscopy.

As these cells have much lower surface phosphatase activity, this finding confirms the proposed enzyme catalyzed fiber formation. Interestingly, subsequent to fiber formation around the membranes of HeLa cells, the DNA-binding dye DAPI (a nucleus marker) was unable to enter the cells. Untreated HeLa cells readily take up DAPI into the nucleus. Especially given the low molecular weight of DAPI (277 g/mol), this result therefore shows that the transport of molecules over the cell membrane can be severely hampered by the formation of an artificial pericellular hydrogel. Furthermore, it was noticed that the gel around the cells contained large amounts of secretory proteins, preventing these proteins from

entering the culture medium. Overall, the hydrogel effectively blocks transport of even small molecules, which has a profound effect on a variety of cellular processes including migration, adhesion and proliferation.

In a later paper by Pires, Ulijn and co-workers[36] a similar strategy was used to form nano-fibers at the cell membrane of cancer cells, exploiting the self-assembling behavior of an aromatic carbohydrate amphiphile **(Fig. 8)** into nano-fibers.

The experimental design was similar to that of the Xu group. Cleavage of a negatively charged phosphate group from a precursor by surface and secretory phosphatases leads to the localized formation of a hydrogelator. Two cell lines were used in this study, namely SaOs2 and ATDC5, where the former has a high phosphatase expression level and the latter produces much lower levels of phosphatases. It was found that upon the addition of the precursor to the two cell lines, the cell viability of the SaOs2 cancer cells dropped to 10%, whereas the ATDC5 cells were virtually unaffected. This result shows that gel formation around the cells efficiently and specifically kill cancer cells although an exact mechanism for its biological effect was not examined in detail. To confirm that self-assembly was triggered by phophatases, Pierce phosphatase inhibitor was added to the SaOs2 cells. Upon the addition of the inhibitor, the SaOs2 cells were not affected by the precursor, clearly indicating that the mechanism of nano-fiber formation requires surface and extracellular phosphatases. To be able to disentangle the effects of membrane bound and extracellular phosphatases, the activity of each was determined individually. It was found that the membrane bound phosphatase activity differed markedly between the two cell lines (i.e. factor 15-20), whereas the extracellular phosphatese activity only differed by a factor 1.5-2.0. It is therefore highly likely that dephosphorylation by membrane bound phosphatases is the main contributor to the self-assembly of the carbohydrate into nano-fibers in the vicinity of the cellular membranes.

The group of Murayama designed a precursor for self-assembly based on a lipidated peptide **(Fig. 9)**.[37] The protein MMP-7 is involved in tumor metastasis and is capable of cleaving the peptide segment Leu-Ala-Arg-Lys of ER-C16, yielding the gelator G-C16. The use of specific proteases is an interesting development, as this potentially allows for greater cell specificity and rational control over the location of the self-assembled fiber networks. G-C16 self-assembles in aqueous solvents into fibers due to hydrophobic interactions between the alkyl chains and hydrogen bonding of the remaining peptide segment. In contrast, ER-C16 does not self-assemble into fibers (instead, micellar structures are formed) due to the presence of the positively charged amino acids prior to enzymatic cleavage.

To test the toxicity of ER-C16 and G-C16, HeLa cells and microvascular endothelial (MvE) cells were selected, as the former is known to excrete MMP-7, whereas the latter does not. Interestingly, the addition of either compound induced cell death among HeLa cells, whereas only G-C16 was able to significantly reduce the viability of MvE cells. These results indicate that only G-C16 is toxic by itself, whereas the addition of ER-C16 leads to cell death through enzyme triggered gelation. Subsequently, precursor ER-C16 was added to a variety of cancer cells where it showed to be detrimental to the viability of these cells, whereas two healthy cell lines (MvE and PE), that contain much lower levels of MMP-7, remained largely unaffected. Photobleaching experiments on fluorescently labelled fibers were performed to investigate the dynamics of the self-assembled structures. It was observed that fluorescence did not recover for 40 minutes, implicating highly static structures which may limit the transport of biomolecules. Regarding the location of gelation, the authors claim that although MMP-7 is excreted by cells and therefore G-C16 is formed around the cells, that gelation occurs intracellularly. However, confocal images seem to indicate that the fibers reside mainly at the membranes of the cells.

The final example of in situ hydrogelation was not aimed at eliminating malignant cells, instead the goal was to aid the suturing of micrometer size blood vessels.[38] Reconnecting small vessels is typically hampered by their collapse and Schneider and co-workers developed a hydrogel which can be used to widen the vessels pre suturing. The researchers constructed a peptide hydrogelator which forms hydrogels based on β-hairpin interactions. Interestingly, upon applying sheer, the hydrogel dissolves as the peptides unfold. Additionally, the network quickly recovers upon the removal of sheer. These characteristics enabled the researchers to inject the hydrogels into both ends of the cut vessel, widening its diameter and preparing it for suturing. Removal of the hydrogel post suturing was achieved by placing a glutamic acid residue in the core of the peptide. Initially, this amino acid residue was protected by a photolabile group and upon irradiation of the hydrogel, the blocking group was removed and an instable hydrogel network was obtained. When applied in mice, excellent blood flow through the sutured vessel was observed post light irradiation.

Overall, the strategy of constructing self-assembled fibrous networks specifically inside or around cancer cells has shown to be a very interesting approach to develop anti-cancer therapies. However, a few issues need attention, including the elucidation of how exactly fiber formation induces apoptosis and a rational approach to control the location of the fiber network (intracellular or at the membrane).

3.3 Therapeutic peptide amphiphile fibers

The use of peptides in materials chemistry has been extremely rewarding, as their intermolecular interactions can be tailored for the formation of ordered structures on the nanoscale through self-assembly.[3a, 39] Peptide amphiphiles typically consist of a hydrophilic peptide which is covalently conjugated to a single alkyl tail. Usually, amphiphiles that have one alkyl tail self-assemble into spherical micelles, however, as the peptides typically contain a beta-sheet domain close to the alkyl chain, extended fibers are often formed. The peptide-peptide interactions can thus be tuned to control the overall morphology of the aggregates.

Additional amino acids can be incorporated, forming the corona of the fibers and thereby enabling control over interactions of the peptide amphiphile fibers with cellular membranes or proteins, through for example binding epitopes or charges on the fiber. We will discuss recent studies that have investigated peptide amphiphile fibers as bioactive materials, mainly studying their cell toxicity, bio distribution upon in vivo injection and delivery of therapeutic peptides. In contrast to the preceding section, the peptide amphiphile fibers discussed here are formed ex vivo and do not form gel networks. Progress regarding tissue engineering applications of peptide amphiphiles will not be discussed as an excellent recent review is available.[9]

In an interesting contribution, the group of Stupp has investigated the influence of the cohesive forces within peptide amphiphile (PA) nanofibers on their toxicity to mammalian cells.[40] To study the effect of intra-fiber hydrogen bonding, two peptide amphiphiles were designed **(Fig. 10)**.

Both **PA1** and **PA2** contain a C_{16} hydrophobic tail which induces aggregation of the PAs upon dispersion in aqueous solutions. Furthermore, both peptide amphiphiles contain three lysine residues at the C-terminus, supplying positive charge to the peptide construct, which enable electrostatic interactions between the PA fibers and negatively charged cellular membranes. Whereas **PA1** contains glycine residues in its core, **PA2** contains valine which promotes beta-sheet formation. Upon the addition of **PA1** to cultured MC3T3-E1 cells, the cell viability was strongly reduced. Importantly, both the peptide segment alone and the anionic analogue of **PA1** were found to be non-toxic. Furthermore, decreasing the alkyl tail (from 16 to 12 carbon atoms) and the removal of one lysine residue reduced cell toxicity. Interestingly, **PA2** was found to be non-toxic, notwithstanding the similar self-assembled architecture. The authors hypothesized that the reduced toxicity was due to stronger intermolecular interactions between the peptide strands. Although no direct investigation was performed to confirm this, X-ray and electron paramagnetic resonance (EPR) measurements did reveal that **PA2**

exhibited strong and stable H-bonds whereas **PA1** showed more dynamic and diffuse scattering patterns.

In another contribution by the Stupp group, peptide amphiphiles that self-assembled into pH sensitive fibers and micelles were investigated for their toxicity towards cancer cells, their ability to encapsulate drugs, and their biodistribution upon injection in mice **(Fig. 10, PA3** and **PA4)**.[41] Due to the alkyl tail and OEG chain, these molecules are amphiphilic and are expected to self-assemble in aqueous solutions. As the imidazole side chain of the histidine residues has a pK_a of 6.0, it was anticipated that slightly acidic conditions would disrupt beta-sheet hydrogen bonding in both peptide amphiphiles and therefore lead to disassembly. Although similar in design, **PA3** self-assembled into fibers, whereas **PA4** formed spherical micelles at pH 7.5. Cryo-TEM and SAXS data showed that upon lowering the pH to 6.0, both **PA3** and **PA4** assemblies dissolved. To examine the pH sensitivity of the toxicity of these two assemblies towards cancer cells, the compounds were added to cultured MDA-MB cells using different pH. Interestingly, **PA3** fibers (pH 7.5) were found to be non-toxic, whereas the monomers (pH 6.0) were highly toxic. It is likely that the positive charge at pH 6.0 enables peptide amphiphile membrane interactions, whereas the neutral fibers are relatively stable and therefore inert. Remarkably however, **PA4** showed the reverse trend, displaying no toxicity at pH 6.0 and slight toxicity at pH 7.5. The difference in toxicities of the spherical micelles **(PA4)** vs the fibers **(PA3)** suggest that the morphology of the self-assembled structure has an influence on its interactions with biological membranes, although detailed investigations are required to unravel its mechanistic underpinnings. Moreover, why the positively charged **PA3** monomers are toxic and the **PA4** monomers are not is unclear. Finally, solutions containing **PA3** and **PA4** were injected into tumor bearing mice, enabling the study of the influence of aggregate morphology on the biodistribution of these PAs. Here, the morphology had a large effect, with the fibrous **PA3** assemblies ending up mainly in the kidneys, liver and tumor, whereas the micellar **PA4** assemblies accumulated predominantly in the liver (12h after

injection). These results show that the clearance and circulation behavior depend heavily on size and morphology of the self-assembled materials where smaller particles are less stable and more prone to filtration by the renal system.

The Stupp group have developed a peptide amphiphile that contains a peptide $(KLAKLAK)_2$ which is covalently coupled to a C_{16} alkyl tail.[42] As the peptide sequence is highly positively charged, it has potential as an antitumor therapeutic, as cancer cells contain more negative charge than healthy cells. The KLAK PA self-assembles into fibers upon dispersion in aqueous solvent, as shown by TEM imaging. To determine the toxicity of this peptide amphiphile towards cancer cells, the assemblies were added to breast cancer cells. Whereas the IC_{50} value of the PA is in the micromolar range, the peptide by itself was found to be non-toxic. As the PA fibers contain high local concentrations of the $(KLAKLAK)_2$ peptide at the fiber surface, this is likely to aid membrane lysis, which has been found to be the mechanism causing toxicity. In a follow up paper,[43] the KLAK PA was mixed with a PA that contained an alkyl tail, a neutral peptide and a PEG chain, yielding PEG PA. PEG is well known to exhibit a screening effect, preventing degradation of the therapeutic peptide, as well as silencing effect, preventing inflammatory responses. Interestingly, the mixed assemblies (1:1 KLAK PA/PEG PA) showed better resistance against proteolytic hydrolysis, whereas the efficacy against cancer cells was retained. Finally, the mixed assembly was added to tumor bearing mice. It was observed that both KLAK PA and the KLAK/PEG PA administration leads to significantly smaller tumors than the control group. This mixed PA system elegantly reveals one of the major strengths of self-assembly, that new material characteristics can be easily developed by mixing two or more components. As observed here, uniform assemblies can be formed using mixtures of assemblies. In future work, it will perhaps be possible to design and develop mixed assemblies with multiple functionalities, leading to more sophisticated interventions in biological processes and accurately directing cellular behavior.

An in-depth investigation concerning the stability, biodistribution and toxicity of L/D-peptide fibers was undertaken by Ding, Kong, Liu and co-workers.[44] In this investigation, two self-assembling peptides were studied, nap-GFFYGRGD (L-peptide) and nap-G^{D}F^{D}F^{D}YGRGD (D-peptide). TEM analysis revealed that both peptides self-assembled into fibers. When the fibers were formed in blood plasma, the D-peptide fibers showed to be remarkably stable for up to 24h, whereas the density of L-peptide fibers decreased strongly over the same period of time. Next, the in vivo stability of the fibers was assessed. The fibers were stained with nile blue and were injected in healthy mice. Upon the collection of a blood sample 0.5 and 1h after the injection, a number of D-peptide fibers could be identified using confocal microscopy, whereas no L-peptide fibers were observed. After 6h post injection however, no D-fibers could be observed and the biodistribution of the fibers was subsequently investigated through analysis of gamma radiation emitted by a ^{125}I label attached to the tyrosine residue of both peptides. Remarkably, the chirality of the peptide fibers had a dramatic effect on the fate of these self-assembled structures. Whereas the D-fibers mainly end up in the liver, the L-fibers reside predominantly in the stomach. Importantly, after 12h, both types of fibers were cleared from the mice, revealing fast metabolic degradation. The transient nature of the self-assembled structures indicate that build-up of toxic effects due to recurrent administrations is not to be expected. Next, the authors administered the fibers to healthy mice via i.v. for 5 consecutive days and the toxicity was evaluated. A library of biochemical indicators were monitored to investigate potential damaging effects. It was found that both L- and D-fibers did not cause altered liver and kidney function and did not spark inflammatory responses.

The group of Uchegbu constructed a peptide amphiphile that can be used to deliver therapeutic peptides across the blood-brain-barrier (BBB).[45] A model peptide called dalargin (Tyr-D-Ala-Gly-Phe-Leu-Arg) was covalently conjugated to a palmitoyl moiety through an ester link. As shown through TEM measurements, these peptide amphiphiles self-assembled into fibrillar aggregates. Remarkably, whereas dalargin itself is rapidly degraded in plasma,

LCMS analysis revealed that the peptide amphiphiles could be traced in plasma, liver and more importantly, the brain. Moreover, concentrations were sufficient to elicit a pharmacological response. To explain these findings, X-ray, linear dichroism (LD) and molecular dynamics simulations were employed on these peptide amphiphile fibers. The authors found that the peptide moiety is wrapped tightly around the core of the fibers, thereby protecting it from degradation. Overall, the results show that these peptide amphiphiles are capable of crossing the BBB, functioning as a reservoir of therapeutic peptides which can be released through the hydrolysis of the ester linkage by esterases.

The examples described in this section show the versatility and (to a large extent) programmability of self-assembling peptides. Based on the amino acid sequence, the inter peptide interactions can be controlled, enabling control over fiber membrane interactions. Furthermore, the hydrophilicity and charge can be tuned, for example controlling whether the peptides are taken up by cells or able to disturb cellular membranes.

3.4 Amphiphilic drug conjugates for drug delivery

In the biomedical field, the efficient delivery of therapeutics is one of the main challenges. Central issues in this field are the poor water solubility of many drugs, enzymatic drug degradation and rapid removal of drugs from the bloodstream. In solving these issues, the use of carriers such as liposomes,[46] polymeric nanoparticles[47] and inorganic materials[48] has been very popular over recent decades. However, these carriers suffer from significant drawbacks, most importantly low drug loading capacity (typically 2-5 weight%) and side effects (e.g. toxicity and inflammation) in the course of degradation, metabolism and excretion of the carriers. In the last few years, an alternative drug delivery strategy based on the controlled self-assembly of drug conjugates into nano aggregates has been developed. By covalently linking drug molecules to a hydrophilic/ self-assembling segment[49] (e.g., a peptide or a gelator), controlled self-assembly yields aggregates that contain up to 50 weight% drug, shield the drug from proteolytic degradation and prolong the residence time in

the bloodstream. Interestingly, based on the overall molecular structure, various aggregate morphologies and particle sizes can be obtained, which are known to influence cellular uptake. Furthermore, (bio)degradable linkers can be used in between the drug and the hydrophilic segment, allowing for the targeted release of the drug based on enzymatic action. In the remainder of this section, the molecular details and efficacy of this approach will be evaluated using recent literature examples.

The group of Cui first investigated the self-assembly of drug-peptide conjugates and their properties in a biological environment.[50] The hydrophobic anticancer drug camptothecin (CPT) was conjugated to a β-sheet forming peptide via a degradable linker (disulfylbutyrate, buSS). Based on this basic design, three derivatives were synthesized, containing 1, 2 and 4 CPT units **(Fig. 11A)**. Accordingly, the drug-peptides contain 23, 31 and 38 weight% drug content, revealing one of the main advantages of this approach over traditional carrier methodologies in which the loading is typically limited to 2-5 weight%. Upon the dispersion of these conjugates in aqueous solution, self-assembly into fibers occurred for all compounds with a CPT core and a peptide corona **(Fig. 11B)**.

Interestingly, the fibers became shorter as the number of CPT molecules increased. Furthermore, the stability of the aggregates increased as a function of the drug content, which is likely due to the increased number of π-π interactions between the CPT units. As the drug units are shielded by the peptide segments, self-assembly here acts to prevent degradation of the drug. Furthermore, release of the drug via the reduction of the disulfylbutyrate can potentially be controlled via the stability of the assemblies. The authors show that addition of GSH to the self-assembled materials resulted in slow release of CPT when tetraCPT was used and fast release when diCPT or monoCPT were used. Interestingly, upon the addition of the self-assembled structures to three cancer cell lines (MCF-7, 9L and F98L), the diCPT derivative showed the highest efficacy followed by the tetraCPT and finally monoCPT. Quite likely, the efficacy of the compounds is complex function of, amongst others, the

hydrophilic/hydrophobic ratio. This ratio controls both the cellular uptake of the drug-peptide conjugates as well as the stability of the self-assembled structures and the resulting shielding of the drug and degradation rate. TetraCPT is likely taken up readily by the cells due to its hydrophobic nature, however the linker is protected from degradation by GSH due to the high stability of the self-assembled structures. Therefore, the intermediate structure diCPT shows the most efficacy as an anti-cancer therapy. Although none of the drug-peptide conjugates were as effective against cancer cells as pure CPT under these conditions, it is possible that in vivo performance would fare better against the pure drug based on half-life times and cellular uptake.

To improve the efficacy of the drug amphiphiles, the Cui group published a follow-up paper in which the linker moiety was tuned, aiming towards the optimization of the anti-cancer efficacy of the drug-peptide conjugates. By exchanging the disulfylbutyrate for a carbonate-based linker, the rate of CPT release was increased, restoring the efficacy of the pure drug.[51] In an additional contribution, the peptide was covalently conjugated to the hydrophobic anticancer drug paclitaxel, linked by a GSH sensitive linker.[52] Self-assembly of this conjugate into fibers was observed and the efficacy of these assemblies against three cancer cell lines was tested. Compared to the pure drug, the drug amphiphiles showed similar cell viabilities under cell culture conditions.

In a following work, the Cui group explored a different self-assembled material for the local delivery of anti-cancer therapeutics. Again, CPT was used as the hydrophobic drug. Here however, cationic and anionic drug conjugates were synthesized, using a beta-sheet forming peptide which was end capped with either two lysine (positive) or two glutamic acid (negative) residues.[53] Furthermore, the CPT and peptide segments were linked via a reducible disulfide linker, allowing for the release of the drug upon reduction by GSH. Amphiphiles containing one, two and four CPT residues were synthesized of which the tetra functionalized amphiphiles (qCPT-Sup35-K2/E2) were of most interest, containing 36% drug

loading. Upon the mixing of these amphiphiles (1:3 molar ratio of amines vs carboxylic acids, respectively) in a 1:1 mixture of MeCN and H_2O, tubular structures were observed with a width of approximately 100 nm and several micrometers in length. The individual amphiphiles however, assembled into fibrous architectures of roughly 6 nm in with. Since the zwitterionic tubes contain 36% anti-cancer drug which could be released after cleavage of the disulfide bond, these self-assembled structures could act as a reservoir of drug molecules with a slow release. To test the in vivo efficacy of this drug delivery vehicle, solutions of this material were injected into tumors present in mice. It was observed through fluorescent labelling of the tubes with Cy7.5 that a significant amount of the self-assembled materials resided in the tumor tissue for more than 36h, whereas the free fluorescent probe eliminated much more rapidly. Although these results are preliminary and did not fully investigate the efficacy of the amphiphilic drug architectures or show release of the rug in vivo, they do show potential for these catanionic nanotubes to act as resistant and stable reservoirs of CPT, which could potentially be beneficial for local tumor treatment.

In an exciting contribution of the Liu group, camptothecin was incorporated in a block-copolymer, yielding a so-called polyprodrug amphiphile.[54] To achieve this design, CPT was covalently modified with a polymerizable methacrylate handle via a disulfide linker. Via a RAFT polymerization, this compound was polymerized from a PEG segment. Self-assembly of the resulting block-copolymer **(Fig. 12)** was initiated by first dissolving the block-copolymer in organic solvent, followed by the slow addition of water. Remarkably, through the choice of organic solvent and the rate of water addition, four distinct assembly morphologies could be accessed: disks, staggered lamellae, large compound vesicles (LCVs) and spherical nanoparticles **(Fig. 12)**. In the method of preparing particles by dissolving the molecules in organic solvent only to slowly add the aqueous solvent later, it is not completely clear whether these particles are formed through true self-assembly, or rather a precipitation-type process. Here, one would need to know the molecular scale packing of the molecular

components within the particles. Such data is not available at this point however and therefore, it remains unclear whether these particles are truly self-assembled aggregates. Nonetheless, in this example and a few others that follow, the shape and size of the observed particles are what would be expected from a typical self-assembly process, given the chemical and physical properties of the used amphiphiles.

All assemblies contain over 50 weight% drug and to investigate the influence of their morphology, uptake of the self-assembled materials by HepG2 cells was studied. Interestingly, both the staggered lamellae and the LVCs entered cells avoiding endocytosis. Accordingly, the entire cytoplasmic region was accessed by these self-assembled structures. In contrast, both the smooth disks and spheres entered cells through endocytosis and consequently these assemblies were trapped in endosomes and lysosomes during the early stages of incubation. Due to the reductive environment inside living cells, the authors investigated intracellular drug release by implementing fluorescent probes in the polymer backbone as well as the CPT unit. Upon incubation of the smooth disks, staggered lamellae and LVCs with the cells, disulfide reduction resulted in clear separation of these fluorophores revealing the fate of CPT to be mainly in the cell nucleus and the polymer backbone to remain in the cytosol. Importantly, the toxicity of the assemblies to cancer cells, with the exception of the spheres, were comparable to pure CPT. In a final investigation, the in vivo blood stability of the assemblies was tested by injecting them into healthy rats. Importantly, cytosolic GSH concentrations are in the mM range, whereas blood plasma contains only μM concentrations of GSH. Consequently, the half-life times of the self-assembled structure were quite long. Moreover, the half-life times of the staggered lamellae (7.62 h) were found to be significantly longer than those of the smooth disks (2.92h) and the LVCs and spheres (<1h), showing their superior stability.

An interesting approach to use self-assembly of a drug molecule for drug delivery purposes was put forth by Zhu, Yan and coworkers. In their work two anti-cancer therapeutic agents

(i.e., irinotecan and chlorambucil) were covalently linked through a hydrolyzable ester bond.[55] As irinotecan is hydrophilic and chlorambucil hydrophobic, the drug conjugate self-assembles in water to form nanospheres of around 100 nm in diameter. Next, the cell viability of irinotecan-chlorambucil was determined and compared to free irinotecan, free chlorambucil and a mixture thereof. Interestingly, below the critical aggregation concentration (CAC), the irinotecan-chlorambucil conjugate is outperformed by irinotecan and the irinotecan/chlorambucil mixture. Above the CAC however, the amphiphilic drug conjugate shows increased efficacy against both MCF-7 and HeLa cells. This finding is a strong indication that the self-assembly of the amphiphilic drug into nanoparticles aids their cellular uptake and overall efficiency. Next the efficiency of irinotecan-chlorambucil against multidrug resistant (MDR) cells (MCF-7/ADR) was evaluated. Generally, nanoparticles are able to prevent active efflux (i.e., active removal of therapeutic agents from cells, as displayed by MDR cells). Whereas the uptake of free irinotecan was reduced by a factor of 50 or 60 in MDR cells, cellular uptake of the irinotecan-chlorambucil conjugate was only reduced by a factor of 2, showing effective resistance against efflux of the irinotecan-chlorambucil aggregates. This result was confirmed when IC_{50} values of irinotecan-chlorambucil and the free drugs were determined for MCF-7 and MCF-7/ADR cells. Whereas the MDR cells only increased the IC_{50} of the aggregates from 13 μM to 15 μM, the free drugs show IC_{50} values that increased 20 times due to active expelling of the drugs. In subsequent studies, mice were injected with either the amphiphilic irinotecan-chlorambucil or the free drugs. First, it was shown that the retention time is significantly enhanced due to the self-assembly of irinotecan-chlorambucil into nano aggregates as compared to the free drugs. Consequently, the efficacy of the amphiphilic drug conjugate against tumors was much higher as compared to the free drugs, as the tumor volume was roughly twice smaller than for the irinotecan/chlorambucil mixture and roughly three times smaller than in the negative control group.

Block copolymer assembly is widely applied for therapeutic and diagnostic purposes.[56] Recently, Gianneschi and co-workers devised an interesting self-assembly based approach to selectively deliver paclitaxel to tumor tissue.[57] The researchers constructed an amphiphilic block co-polymer that contained paclitaxel (hydrophobic) and a peptide (hydrophilic) that is recognized and cleaved by matrix metallo proteinases, which are overexpressed in cancer cells. This compound self-assembled into micelles, bearing the peptide moieties at their exterior. Upon diffusion into cancer cells, the peptide units were removed and large self-assembled structures were formed. Once this occurs, the self-assembled structures are trapped within the malignant cells. As paclitaxel was covalently attached to the polymer via an ester bond, subsequent hydrolysis of this bond yields the free drug. The efficacy of the MMP responsive nanoparticles was tested in mice and the authors showed that the materials ended up mainly in the tumour tissue and that nanoparticle efficacy against cancer cells was comparable to paclitaxel alone. However, whether this effect was only due to release of the drug, or also caused by the increase in size of the aggregates was not determined.

Overall, the use of amphiphiles containing therapeutic agents that self-assemble into stable aggregates shows great potential as drug delivery devices. This strategy has advantageous characteristics of nanoparticle drug delivery vehicles such as protection of the drug against proteolytic degradation and expanded lifetime in the bloodstream. Furthermore, the main advantage of drug self-assembly over drug carriers is the high loading, with typically 2-5% for drug carriers and up to 50% for the drug amphiphiles. Additionally, the efficacy of the amphiphilic drugs against cancer cells could be improved by incorporating a cleavable linker in the design, releasing the drug upon enzymatic action.

4. Conclusions and outlook

The work discussed in this progress report illustrates that self-assembly of synthetic molecules has tremendous potential for the formation of bioactive materials and that this emerging field might well become a key area in chemical biology and medicine. Whereas

traditional therapeutics and imaging tools are typically based on the action of individual molecules, self-assembly based approaches aim towards the formation of ordered bioactive materials. The formation of such nano aggregates enables important prospects, ranging from the protection of drugs from degradation to the concentration and localization of fluorescence leading to highly efficient imaging materials. Moreover, self-assembly enables straightforward functionalization of the surface of aggregates with bioactive epitopes, which enhances their interaction with the biological material. For instance, by simply mixing various functionalized amphiphiles it is possible to design assemblies with different functional groups at their surface at precisely controlled concentrations and ratios. As the aggregates are held together by interactions of similar strength as many biological supramolecular constructs (e.g. cell membranes, or the extracellular matrix), they are potentially capable of interacting with self-assembled organelles or membranes, changing their structure and function. Moreover, the formation of intracellular fiber networks can lead to a decrease in the metabolic activity of cells. If the location of such fiber networks can be precisely controlled and functionalized, even more sophisticated medical applications of this basic scheme might be feasible. The functionalized network could then possibly act as a reservoir of functional groups, capable of binding harmful DNA/RNA sequences or proteins, so as to selectively deactivate them.

Clearly, controlling the location where self-assembly takes place is a major challenge. We have observed that the triggers that spark self-assembly are mainly limited to enzymatic cleavage of a self-assembly blocking group. It seems likely that the near future will witness the development of systems in which self-assembly occurs in response to a variety of biological stimuli including chemical gradients, mechanical forces such as pressure or shear, or pH[4] (as cancer cells typically display lower pH than normal tissue). Likewise, external stimuli such as light,[5] magnetic fields or local heating may be used to control local assembly and bioactivity. Furthermore, temporal control over self-assembly is an issue that has not been addressed until now. Towards this aim, out of equilibrium self-assembly might be used to

construct transient structures.[58], [59] These systems require an input of chemical energy (a fuel) to drive transient self-assembly, resulting in the formation of assemblies that dissolve over time as the activated building blocks revert back to the non-self-assembling molecules. In terms of medicine, this translates to the installment of a therapeutic self-assembled structure (e.g., an extracellular fiber network) that dissolves over time once its function is fulfilled.

Acknowledgements

We thank the Netherlands Organization for Scientific Research (NWO VIDI grant to R.E.) for funding.

References

[1] a) S. G. Zhang, Nat. Biotechnol. 2003, 21, 1171; b) T. Aida, E. W. Meijer, S. I. Stupp, Science 2012, 335, 813; c) K. Petkau-Milroy, L. Brunsveld, Org. Biomol. Chem. 2013, 11, 219.

[2] H. Frisch, P. Besenius, Macromol. Rapid Commun. 2015, 36, 346.

[3] a) J. D. Hartgerink, E. Beniash, S. I. Stupp, Science 2001, 294, 1684; b) A. Brizard, M. Stuart, K. van Bommel, A. Friggeri, M. de Jong, J. van Esch, Angew. Chem. Int. Ed. 2008, 47, 2063; c) J. Boekhoven, M. Koot, T. A. Wezendonk, R. Eelkema, J. H. van Esch, J. Am. Chem. Soc. 2012, 134, 12908.

[4] A. Aggeli, M. Bell, L. M. Carrick, C. W. G. Fishwick, R. Harding, P. J. Mawer, S. E. Radford, A. E. Strong, N. Boden, J. Am. Chem. Soc. 2003, 125, 9619.

[5] V. Faramarzi, F. Niess, E. Moulin, M. Maaloum, J.-F. Dayen, J.-B. Beaufrand, S. Zanettini, B. Doudin, N. Giuseppone, Nat. Chem. 2012, 4, 485.

[6] a) Z. Yang, P.-L. Ho, G. Liang, K. H. Chow, Q. Wang, Y. Cao, Z. Guo, B. Xu, J. Am. Chem. Soc. 2007, 129, 266; b) Z. M. Yang, H. W. Gu, D. G. Fu, P. Gao, J. K. Lam, B. Xu, Adv. Mater. 2004, 16, 1440; c) Z. Yang, G. Liang, B. Xu, Acc. Chem. Res. 2008, 41, 315.

[7] J. Boekhoven, J. M. Poolman, C. Maity, F. Li, L. van der Mee, C. B. Minkenberg, E. Mendes, J. H. van Esch, R. Eelkema, Nat. Chem. 2013, 5, 433.

[8] a) E. Saxon, C. R. Bertozzi, Science 2000, 287, 2007; b) W. G. Lewis, L. G. Green, F. Grynszpan, Z. Radic, P. R. Carlier, P. Taylor, M. G. Finn, K. B. Sharpless, Angew. Chem. Int. Ed. 2002, 41, 1053; c) Y. Zeng, T. N. C. Ramya, A. Dirksen, P. E. Dawson, J. C. Paulson, Nat. Methods 2009, 6, 207.

[9] J. Boekhoven, S. I. Stupp, Adv. Mater. 2014, 26, 1642.

[10] J. Brinkmann, E. Cavatorta, S. Sankaran, B. Schmidt, J. van Weerd, P. Jonkheijm, Chem. Soc. Rev. 2014, 43, 4449.

[11] B. N. G. Giepmans, S. R. Adams, M. H. Ellisman, R. Y. Tsien, Science 2006, 312, 217.

[12] G. Liang, H. Ren, J. Rao, Nat. Chem. 2010, 2, 54.

[13] J. Shapiro, N. Sciaky, J. Lee, H. Bosshart, R. H. Angeletti, J. S. Bonifacino, J. Histochem. Cytochem. 1997, 45, 3.

[14] G. Liang, J. Ronald, Y. Chen, D. Ye, P. Pandit, M. L. Ma, B. Rutt, J. Rao, Angew. Chem. Int. Ed. 2011, 50, 6283.

[15] D. Ye, G. Liang, M. L. Ma, J. Rao, Angew. Chem. Int. Ed. 2011, 50, 2275.

[16] D. Ye, P. Pandit, P. Kempen, J. Lin, L. Xiong, R. Sinclair, B. Rutt, J. Rao, Bioconjugate Chem. 2014, 25, 1526.

[17] D. Ye, A. J. Shuhendler, L. Cui, L. Tong, S. S. Tee, G. Tikhomirov, D. W. Felsher, J. Rao, Nat. Chem. 2014, 6, 519.

[18] D. Ye, A. J. Shuhendler, P. Pandit, K. D. Brewer, S. S. Tee, L. Cui, G. Tikhomirov, B. Rutt, J. Rao, Chem. Sci. 2014, 5, 3845.

[19] B. Shen, J. Jeon, M. Palner, D. Ye, A. Shuhendler, F. T. Chin, J. Rao, Angew. Chem. Int. Ed. 2013, 52, 10511.

[20] D. Hoekstra, T. Deboer, K. Klappe, J. Wilschut, Biochemistry 1984, 23, 5675.

[21] D. Ding, K. Li, B. Liu, B. Z. Tang, Acc. Chem. Res. 2013, 46, 2441.

[22] H. Shi, R. T. K. Kwok, J. Liu, B. Xing, B. Z. Tang, B. Liu, J. Am. Chem. Soc. 2012, 134, 17972.

[23] H. Shi, N. Zhao, D. Ding, J. Liang, B. Z. Tang, B. Liu, Org. Biomol. Chem. 2013, 11, 7289.

[24] H. Wang, J. Liu, A. Han, N. Xiao, Z. Xue, G. Wang, J. Long, D. Kong, B. Liu, Z. Yang, D. Ding, ACS Nano 2014, 8, 1475.

[25] K. Mizusawa, Y. Takaoka, I. Hamachi, J. Am. Chem. Soc. 2012, 134, 13386.

[26] T. Yoshii, K. Mizusawa, Y. Takaoka, I. Hamachi, J. Am. Chem. Soc. 2014, 136, 16635.

[27] C. Ren, H. Wang, D. Mao, X. Zhang, Q. Fengzhao, Y. Shi, D. Ding, D. Kong, L. Wang, Z. Yang, Angew. Chem. Int. Ed. 2015, 54, 4823.

[28] R. B. Merrifield, J. Am. Chem. Soc. 1963, 85, 2149.

[29] F. Versluis, H. R. Marsden, A. Kros, Chem. Soc. Rev. 2010, 39, 3434.

[30] aJ. Zhou, B. Xu, Bioconjugate Chem. 2015, 26, 987; bM. Hughes, S. Debnath, C. W. Knapp, R. V. Ulijn, Biomaterials Science 2013, 1, 1138.

[31] Z. Yang, G. Liang, Z. Guo, Z. Guo, B. Xu, Angew. Chem. Int. Ed. 2007, 46, 8216.

[32] Z. Yang, K. Xu, Z. Guo, Z. Guo, B. Xu, Adv. Mater. 2007, 19, 3152.

[33] Y. Gao, J. Shi, D. Yuan, B. Xu, Nat. Comm. 2012, 3, 1.

[34] aY. Gao, C. Berciu, Y. Kuang, J. Shi, D. Nicastro, B. Xu, Acs Nano 2013, 7, 9055; bY. Gao, Y. Kuang, X. Du, J. Zhou, P. Chandran, F. Horkay, B. Xu, Langmuir 2013, 29, 15191.

[35] Y. Kuang, J. Shi, J. Li, D. Yuan, K. A. Alberti, Q. Xu, B. Xu, Angew. Chem. Int. Ed. 2014, 53, 8104.

[36] R. A. Pires, Y. M. Abul-Haija, D. S. Costa, R. Novoa-Carballal, R. L. Reis, R. V. Ulijn, I. Pashkuleva, J. Am. Chem. Soc. 2015, 137, 576.

[37] A. Tanaka, Y. Fukuoka, Y. Morimoto, T. Honjo, D. Koda, M. Goto, T. Maruyama, J. Am. Chem. Soc. 2015, 137, 770.

[38] D. J. Smith, G. A. Brat, S. H. Medina, D. Tong, Y. Huang, J. Grahammer, G. J. Furtmüller, B. C. Oh, K. J. Nagy-Smith, P. Walczak, G. Brandacher, J. P. Schneider, Nat Nano 2016, 11, 95.

[39] a) J. B. Matson, S. I. Stupp, Chem. Commun. 2012, 48, 26; b) S. Cavalli, F. Albericio, A. Kros, Chem. Soc. Rev. 2010, 39, 241.

[40] C. J. Newcomb, S. Sur, J. H. Ortony, O.-S. Lee, J. B. Matson, J. Boekhoven, J. M. Yu, G. C. Schatz, S. I. Stupp, Nat. Comm. 2014, 5.

[41] T. J. Moyer, J. A. Finbloom, F. Chen, D. J. Toft, V. L. Cryns, S. I. Stupp, J. Am. Chem. Soc. 2014, 136, 14746.

[42] D. J. Toft, T. J. Moyer, S. M. Standley, Y. Ruff, A. Ugolkov, S. I. Stupp, V. L. Cryns, Acs Nano 2012, 6, 7956.

[43] S. M. Standley, D. J. Toft, H. Cheng, S. Soukasene, J. Chen, S. M. Raja, V. Band, H. Band, V. L. Cryns, S. I. Stupp, Cancer Res. 2010, 70, 3020.

[44] C. H. Yang, L. P. Chu, Y. M. Zhang, Y. Shi, J. J. Liu, Q. Liu, S. J. Fan, Z. M. Yang, D. Ding, D. L. Kong, J. F. Liu, ACS Appl. Mater. Inter. 2015, 7, 2735.

[45] M. Mazza, R. Notman, J. Anwar, A. Rodger, M. Hicks, G. Parkinson, D. McCarthy, T. Daviter, J. Moger, N. Garrett, T. Mead, M. Briggs, A. G. Schaetzlein, I. F. Uchegbu, Acs Nano 2013, 7, 1016.

[46] V. P. Torchilin, Nat. Rev. Drug Disov. 2005, 4, 145.

[47] J. Nicolas, S. Mura, D. Brambilla, N. Mackiewicz, P. Couvreur, Chem. Soc. Rev. 2013, 42, 1147.

[48] F. Tang, L. Li, D. Chen, Adv. Mater. 2012, 24, 1504.

[49] a) K. J. C. van Bommel, M. C. A. Stuart, B. L. Feringa, J. van Esch, Org. Biomol. Chem. 2005, 3, 2917; b) B. G. Xing, C. W. Yu, K. H. Chow, P. L. Ho, D. G. Fu, B. Xu, J. Am. Chem. Soc. 2002, 124, 14846; c) Y. Gao, Y. Kuang, Z.-F. Guo, Z. Guo, I. J. Krauss, B. Xu, J. Am. Chem. Soc. 2009, 131, 13576.

[50] A. G. Cheetham, P. Zhang, Y.-a. Lin, L. L. Lock, H. Cui, J. Am. Chem. Soc. 2013, 135, 2907.

[51] A. G. Cheetham, Y.-C. Ou, P. Zhang, H. Cui, Chem. Commun. 2014, 50, 6039.

[52] R. Lin, A. G. Cheetham, P. C. Zhang, Y. A. Lin, H. G. Cui, Chem. Commun. 2013, 49, 4968.

[53] Y.-A. Lin, A. G. Cheetham, P. Zhang, Y.-C. Ou, Y. Li, G. Liu, D. Hermida-Merino, I. W. Hamley, H. Cui, Acs Nano 2014, 8, 12690.

[54] X. Hu, J. Hu, J. Tian, Z. Ge, G. Zhang, K. Luo, S. Liu, J. Am. Chem. Soc. 2013, 135, 17617.

[55] P. Huang, D. Wang, Y. Su, W. Huang, Y. Zhou, D. Cui, X. Zhu, D. Yan, J. Am. Chem. Soc. 2014, 136, 11748.

[56] M. Elsabahy, G. Seong Heo, S.-M. Lim, G. Sun, K. L. Wooley, Chem. Rev. 2015, 115, 10967−11011.

[57] C. E. Callmann, C. V. Barback, M. P. Thompson, D. J. Hall, R. F. Mattrey, N. C. Gianneschi, Adv. Mater. 2015, 27, 4611.

[58] a) S. Debnath, S. Roy, R. V. Ulijn, J. Am. Chem. Soc. 2013, 135, 16789; b) J. Boekhoven, A. M. Brizard, K. N. K. Kowlgi, G. J. M. Koper, R. Eelkema, J. H. van Esch, Angew. Chem. Int. Ed. 2010, 49, 4825.

[59] J. Boekhoven, W. E. Hendriksen, G. J. M. Koper, R. Eelkema, J. H. van Esch, Science 2015, 349, 1075.

Received: ((will be filled in by the editorial staff))
Revised: ((will be filled in by the editorial staff))
Published online: ((will be filled in by the editorial staff))

Images

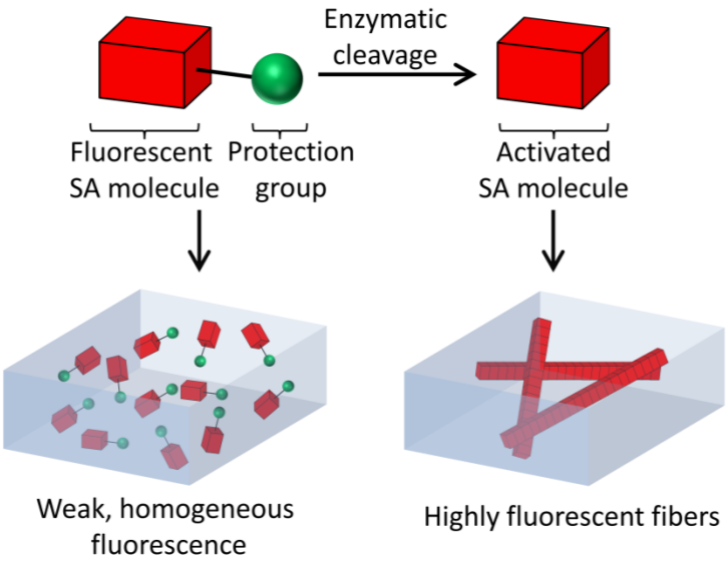

Figure 1. Schematic representation of enzyme triggered self-assembly of a fluorescent molecule in aqueous media. Before cleavage of the self-assembly blocking group, weak homogeneous fluorescence is observed. Upon enzyme triggered self-assembly however, strongly fluorescent materials are observed in the vicinity of the enzyme.

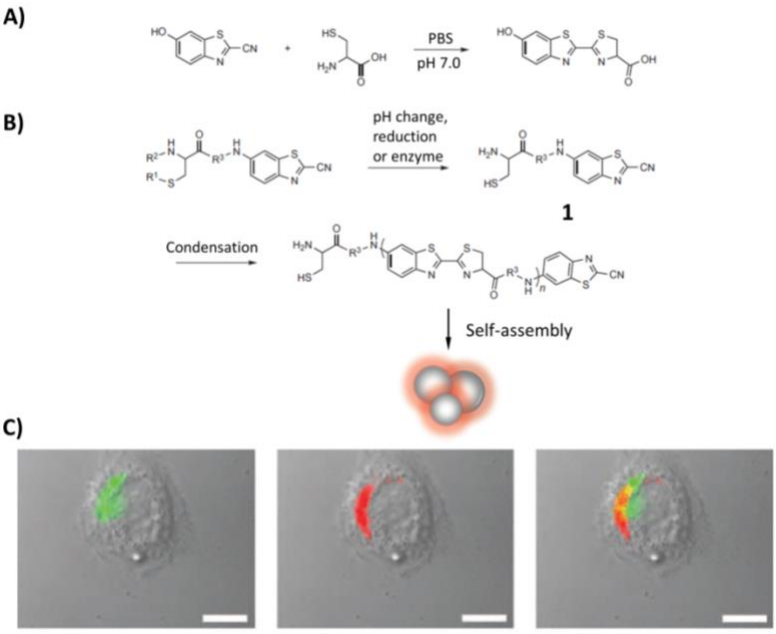

Figure 2. A) Scheme of controlled condensation between 2-cyanobenzothiazole and free cysteine. **B)** Proposed two-step condensation of monomers which can be controlled by pH, reduction or an enzyme, leading to self-assembly. **C)** Imaging of furin triggered localized self-assembly in MDA-MB-468 cells, revealing that aggregation takes place near Golgi bodies. Left: an overlay of differential interference contrast (DIC) and fluorescence image of the condensation product. Middle: an overlay of DIC and Golgi staining (DsRed channel). Right: an overlay of previous two images. Scale bars: 10 μm. Adapted with permission.[12] Copyright 2010, Nature Publishing Group.

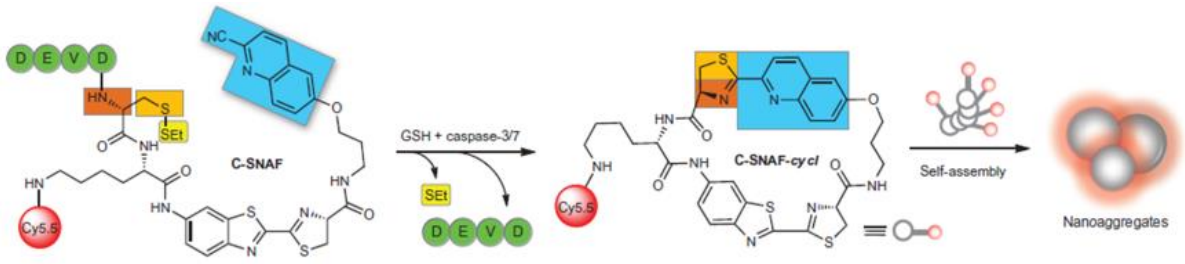

Figure 3. Schematic representation of precursor C-SNAF and the mechanism through which caspase and GSH mediated cleavage of blocking groups leads to the formation of highly

fluorescent nano-aggregates. Adapted with permission.[17] Copyright 2014, Nature Publishing Group.

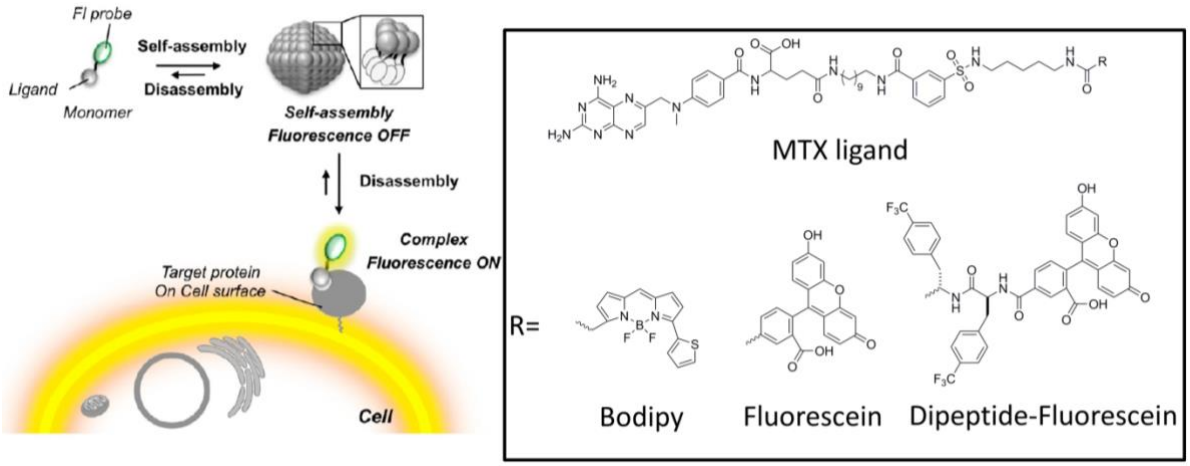

Figure 4. Schematic representation of the (AIQ) based turn on/off probe and its chemical structure. Upon aggregation, the probe is silent, when the target is recognized however, the aggregates disassemble and the fluorescence is turned on. Adapted with permission.[25] Copyright 2012, American Chemical Society.

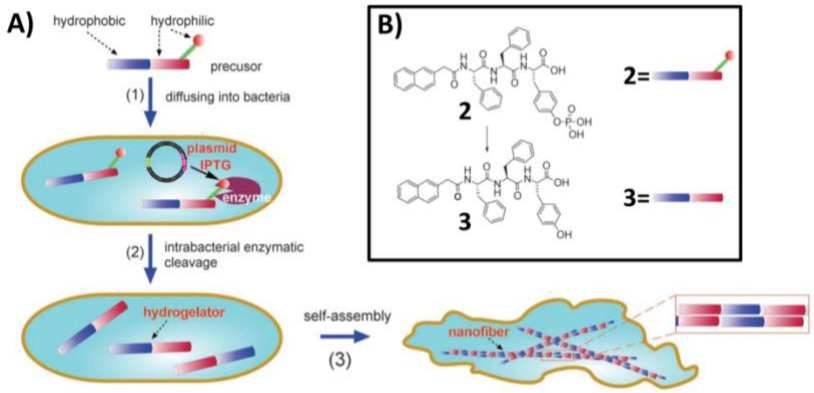

Figure 5. A) Schematic overview of enzyme catalyzed, intrabacterial gelation, leading to inhibition of bacteria. **B)** Molecular structures of the precursor and the hydrogelator. Adapted with permission.[31] Copyright 2014, Wiley-VCH.

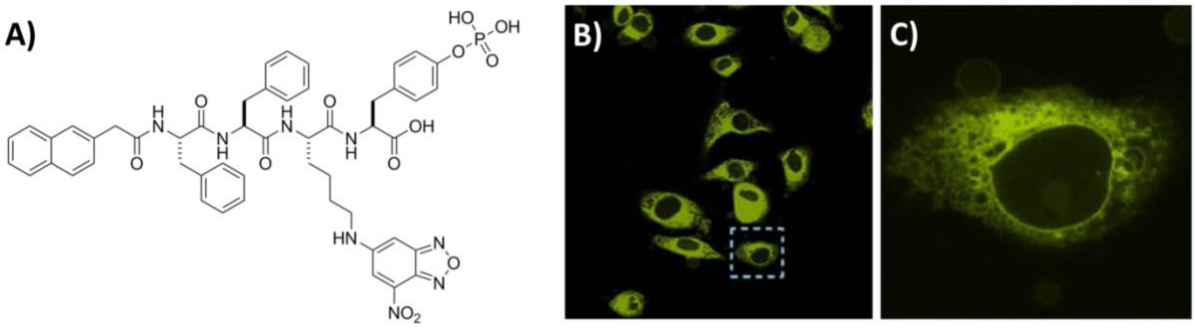

Figure 6. A) Molecular structure of the NBD labelled precursor for hydrogelation. **B,C)** Confocal fluorescence images of HeLa cells, incubated with the fluorescently labelled precursor (imaged after 5 minutes). Adapted with permission.[33] Copyright 2014, Nature Publishing Group

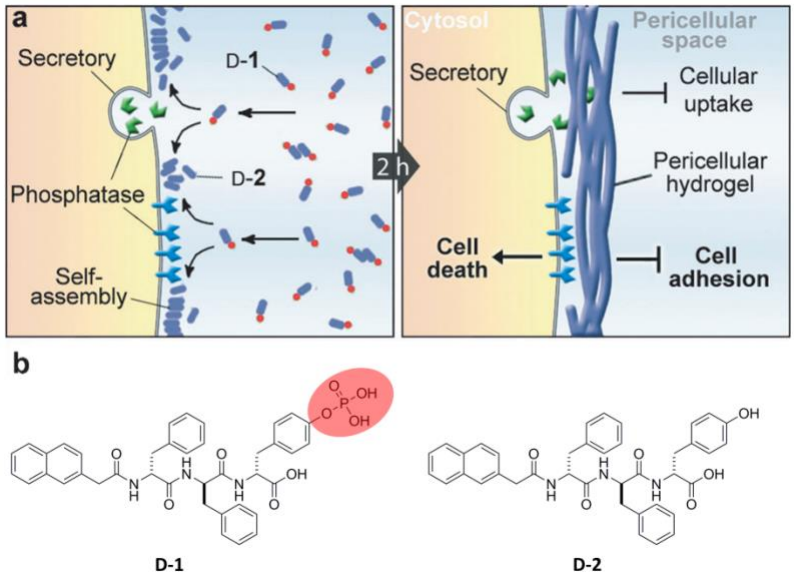

Figure 7. A) Enzyme catalyzed formation of fibers in the vicinity of cellular membranes. **B)** Molecular structures of the precursor for self-assembly (**D-1**) and the self-assembling agent (**D-2**). Reproduced with permission.[35] Copyright 2014, Wiley-VCH.

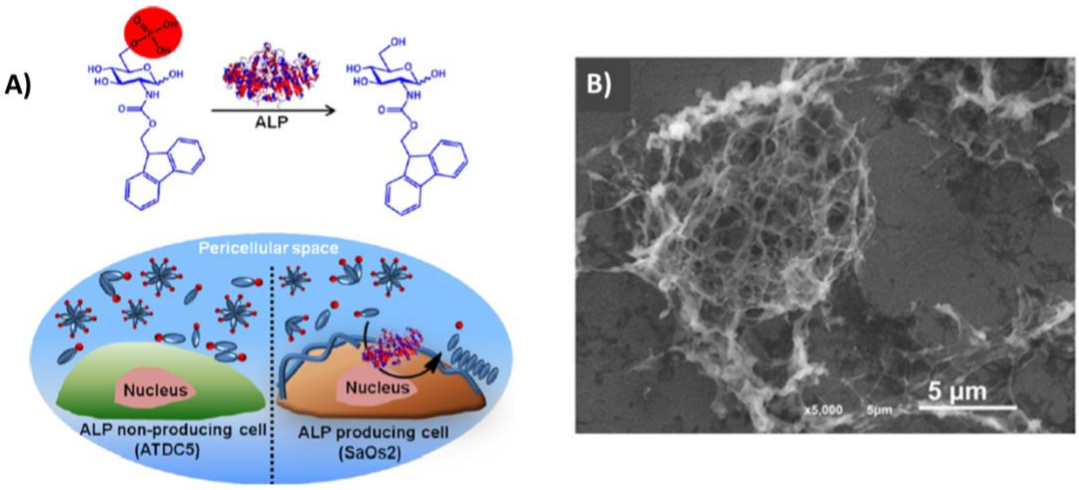

Figure 8. A) Schematic representation of phosphatase triggered self-assembly of an aromatic carbohydrate amphiphile into nano-fibers around the membranes of cancer cells. **B)** SEM image of SaOs2 cells, incubated with the precursor hydrogelator for 7 hours. Adapted with permission.[36] Copyright 2015, American Chemical Society.

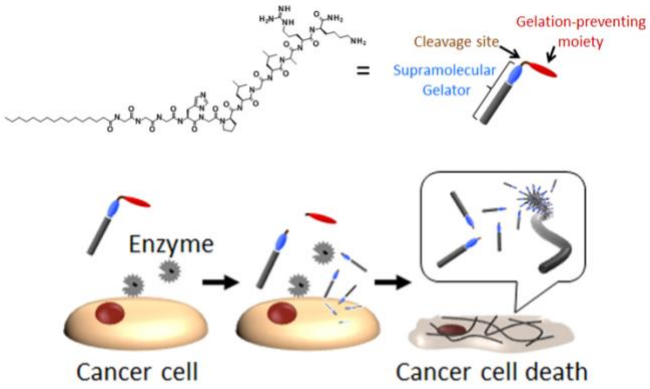

Figure 9. Molecular and schematic structure of the peptide amphiphile precursor. Upon the addition of the precursor to cells, enzymatic cleavage of the peptide leads to fiber formation and gelation at the cellular membrane, inducing cell death. Adapted with permission.[37] Copyright 2015, American Chemical Society.

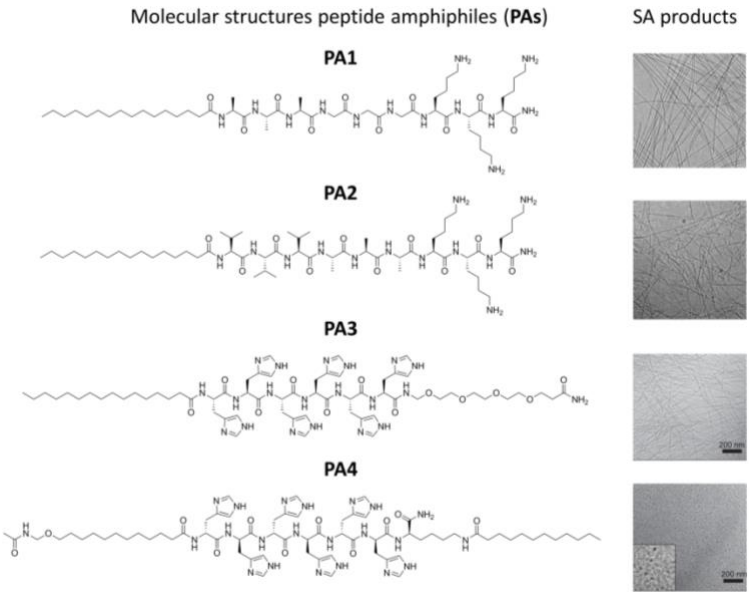

Figure 10. Chemical structures and self-assembly products (cryo-TEM) of PA1, PA2, PA3 and PA4. Adapted with permission.[40-41] Copyright 2014, Nature Publishing Group and American Chemical Society

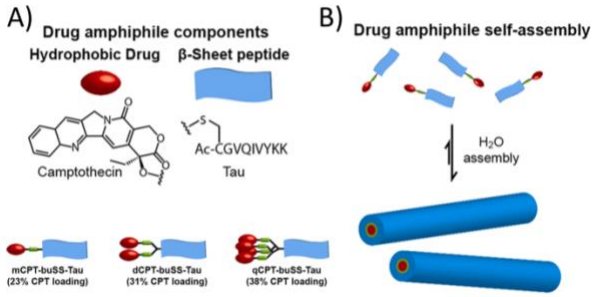

Figuur 11. A) Schematic and molecular illustrations of the drug amphiphiles and **B)** cartoon of fiber formation upon the dispersion of the drug amphiphiles in aqeous media. Adapted with permission.[50] Copyright 2013, American Chemical Society.

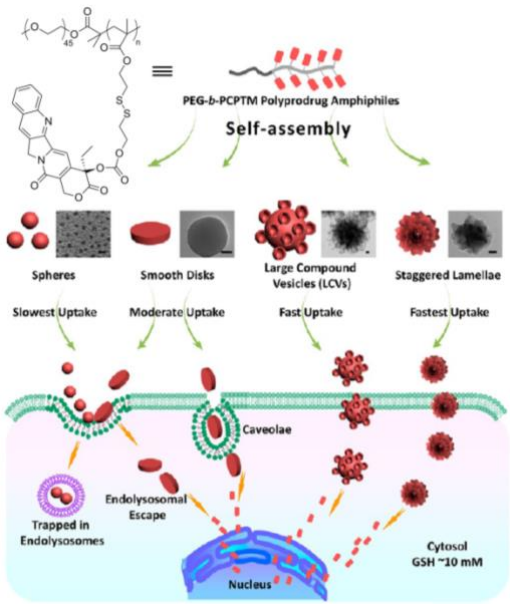

Figure 12. Schematic representation of the polyprodrug copolymer, the various morphologies that could be accessed via self-assembly and the mechanism of cellular uptake of these assemblies. Reproduced with permission.[54] Copyright 2013, American Chemical Society.

Author Biographies

Frank Versluis

Frank Versluis received his PhD degree from Leiden University. There, he worked on a peptide based supramolecular system that functions both ex vivo and in vivo as a tool to deliver hydrophilic compounds across membranes. Currently, Dr. Versluis is a postdoctoral researcher at the laboratory of Dr. Eelkema in the Advanced Soft Matter group at TU Delft. There his main focus is on supramolecular hydrogels and their biological applications.

Jan H. van Esch

Jan H van Esch is professor of chemistry at the Department of Chemical Engineering of the University of Delft, and he chairs the Advanced Soft Matter group. He is a supramolecular and physical organic chemistry scientist from the dutch Nolte school (PhD), and did postdoctoral stays with Helmut Ringsdorf and Ben Feringa. His research focusses on directed self-assembly and far-from-equilibrium phenomena in molecular systems, and to exploit such systems in smart materials and biomedical applications.

Rienk Eelkema

Rienk Eelkema is an assistant professor at TU Delft. He obtained his PhD in chemistry (*cum laude*) with Prof. Ben Feringa. After postdoctoral work at the University of Oxford with Prof. Harry Anderson, he joined the TU Delft Faculty in 2008 (tenured in 2013). His main research

interests include the use of chemical reactivity to control self-assembly processes and soft materials, and the design and synthesis of new materials for applications in physics and biology.

Table of contents entry

Synthetic self-assembly has long been recognized as an excellent approach for the formation of ordered structures on the nanoscale. Since a few years, such self-assembling systems are applied as bioactive materials in biological environments. This progress report is devoted to this up-and-coming field which has the potential of becoming a key area in chemical biology and medicine.

Keywords: Self-assembly, cellular imaging, therapeutics, enzymes, biomaterials

F. Versluis, J. H. van Esch and R. Eelkema

Synthetic Self-Assembled Materials in Biological Environments

ToC figure

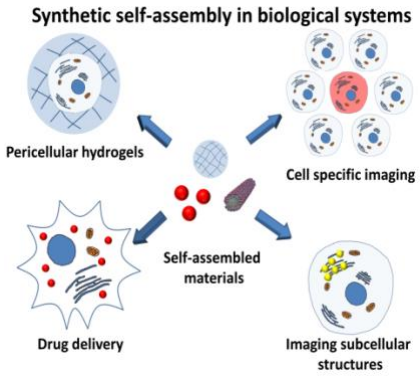
Synthetic self-assembly in biological systems
Pericellular hydrogels
Cell specific imaging
Self-assembled materials
Drug delivery
Imaging subcellular structures